LUBRICATION SCIENCE
Lubrication Science (2012)
Published online in Wiley Online Library (wileyonlinelibrary.com). DOI: 10.1002/ls.1182

Effect of heat treatment on tribological behaviour of welding deposits for hardfacing

Agustín Gualco[1,*,†], Hernán G. Svoboda[2,3], Estela S. Surian[1,4,5] and Luis A. deVedia[6]

[1]*Faculty of Engineering, National University of Lomas de Zamora, Camino de Cintura y Juan XXIII, 1832 Lomas de Zamora, Buenos Aires, Argentina*
[2]*Faculty of Engineering, University of Buenos Aires, Las Heras 2214, 1427 Buenos Aires, Argentina*
[3]*CONICET, Las Heras 2214, 1427 Buenos Aires, Argentina*
[4]*Faculty of Engineering, National University of Lomas de Zamora, Blanco Encalada 4580 12A, 1431 Buenos Aires, Argentina*
[5]*Regional Faculty of San Nicolás, National Technological University, Blanco Encalada 4580 12A, 1431 Buenos Aires, Argentina*
[6]*Institute of Technology Prof. Jorge A. Sabato, National University of San Martín/National Agency of Atomic Energy, Av. Gral. Paz 1499, 1650 Buenos Aires, Argentina*

ABSTRACT

This paper analyses the effects of post-welding heat treatment on the tribological response of weld metals for hardfacing. Applied load in wear tests was also studied. The deposit was a martensitic steel obtained with a gas metal arc welding metal-cored wire under gas shielding of Ar–2% CO_2 and 2 kJ mm^{-1} of heat input. Cross sections were obtained from the welded coupon and subjected at 550°C for 2 h. These samples, together with the as-welded (AW) specimens, constituted the system under study. Cross sections were also extracted for both conditions for determination of chemical composition, microstructure characterisation, microhardness measurements in addition to friction and metal–metal wear tests in pure sliding at 500, 1250 and 2000 N of applied load. A microstructure composed of martensite and retained austenite was observed for both conditions. The AW sample presented 16% of retained austenite, whereas the heat-treated one presented 8%. Heat-treated coupons showed secondary hardening associated with precipitation phenomena. In the specimens tested at 500 and 1250 N, the wear mechanism was oxidative and the AW specimens presented higher wear resistance and higher friction coefficient. On the contrary, the wear regimen of the samples tested at 2000 N was severe, with the heat-treated ones more wear resistant with a higher friction coefficient. Copyright © 2012 John Wiley & Sons, Ltd.

Received 25 April 2011; Revised 9 February 2012; Accepted 10 February 2011

KEY WORDS: hardfacing welding; heat treatment; friction; wear; martensitic steels

INTRODUCTION

The technology of materials has experienced significant progress over the last years, especially in terms of surface coatings, with currently available specific coatings applicable to particular purposes and resistant to different types of demands. In this aspect, the systematic study of consumables and

*Correspondence to: Agustín Gualco, Faculty of Engineering, National University of Lomas de Zamora, Camino de Cintura y Juan XXIII, (1832) Lomas de Zamora, Buenos Aires, Argentina.
†Email: agustingualco@yahoo.com.ar

welding processes applied to hard surfacing is of great interest for the optimisation of the consumable design and for the assessment and tuning of welding procedures. Within this context, heat input, shielding gas composition, pre-heating temperature and post-welding heat treatment are some of the most relevant variables of the welding process.[1]

In recent years, tubular wires have been one of the most used options among the electric arc welding consumables. These consumables are highly productive and flexible for manufacturing of alloy grading, therefore constituting an economical alternative for big productions.[2] Metal-cored wires constitute state-of-the-art consumables with the advantage of a very low slag generation, fume formation reduction and higher deposition rate.[3,4] However, the information available on systematic studies of these types of consumables, especially for reclaiming applications, is very poor.

Generally, the material for wear-resistant applications presents a structure that is very hard or can be made hard by mechanical working or heat treatment, e.g. martensite or a soft matrix with hard particles (carbides and/or borides) according to the intended application.[5] Particularly, for metal–metal sliding or rolling service, where wear is mainly caused by sub-surface fatigue and adhesion, the materials usually used contain carbon from 0.1% to 0.7% and up to 20% alloying (Cr, Mn, Mo, W and/or V) such as martensitic tool steel or stainless martensitic steel.[1,6] These welding deposits often require a post-welding heat treatment. This kind of treatment adjusts final mechanical properties and allows relief of tensions, which are of great importance for the component useful life.[7] Particularly, the chosen alloy for this work was an appropriate one for hot work tools, such as forging dies.

The purpose of this work was to study the effects of both post-welding heat treatment and the applied load in the wear test on tribological behaviour and microstructural evolution of a martensitic steel weld metal. This was obtained with a metal-cored tubular wire welded with gas shielded semi-automatic welding process, in order to better understand the relationships among process variables, microstructural evolution and properties.

MATERIALS AND METHODS

A test coupon consisting of a 375 × 75 mm AISI 1010 carbon steel plate, 19 mm thick, was surfaced by welding. Four layers were deposited with five, four, four and three beads per layer according to the sequence shown in Figure 1a.

The consumable used was a 1.2 mm diameter metal-cored tubular wire depositing a martensitic tool steel. A welding power source for pulsed semi-automatic arc welding ESAB LAI 400P was used with the Railtrac FW1000 Flexi Weaver System (Figure 1b shows this equipment). Welding parameters used are shown in Table I.

The wire stickout was 20 mm, and the gas flow was 20 l min^{-1}. Welding was performed in the flat position with pre-heating and interpass temperatures of 150°C. The quality of the welded coupon was evaluated by radiographic testing.

Twelve 10 mm thick cross sections were obtained from the welded coupon; six of them were subjected to post-welding heat treatment at 550°C for 2 h. This temperature was selected on the basis of a previous work.[8]

The chemical composition was determined on the last bead by optical emission spectroscopy, and local composition was analysed by energy dispersive X-ray spectroscopy (EDS) at different distances from the top surface, since composition is modified due to dilution with the base metal (AISI 1010). The analysed conditions were characterised by light microscopy and X-ray diffraction (XRD). From

DOI: 10.1002/ls

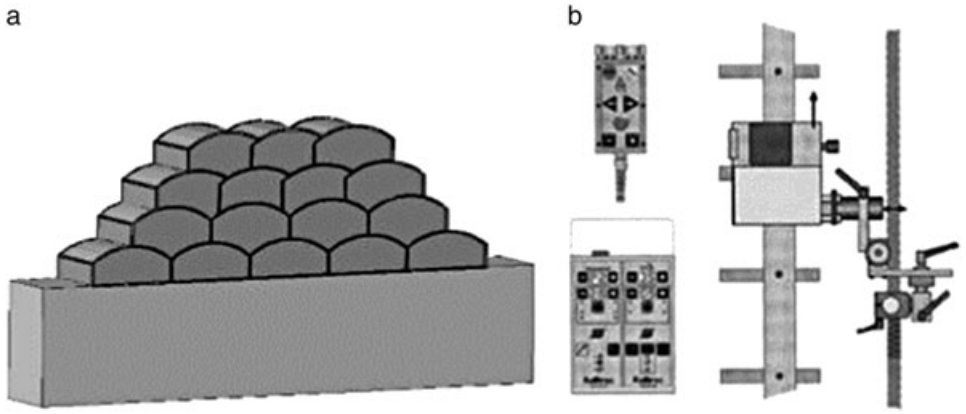

Figure 1. (a) Welding sequence and (b) Railtrac FW1000 system.

Table I. Welding parameters.

Shielding gas	Voltage (V)	Current (A)	Welding speed ($mm\,s^{-1}$)	Heat input ($kJ\,mm^{-1}$)
Ar–2% CO_2	28	180	2.6	1.9

the XRD patterns, the retained austenite fraction was estimated by means of the direct peak comparison method.[9] From the heat-treated and 'as-welded' (AW) samples, specimens were milled for tribological testing, which was conducted with an Amsler machine in conditions of pure sliding with loads of 500, 1250 and 2000 N; the sliding velocity during the test was $0.46\,m\,s^{-1}$. The sample geometry is shown in Figure 2a. AISI 1020 steel was used as a reference material (180 HV1 and $Ra = 0.8\,\mu m$). Before the tests, the samples were ultrasonically cleaned and weighed in an analytical

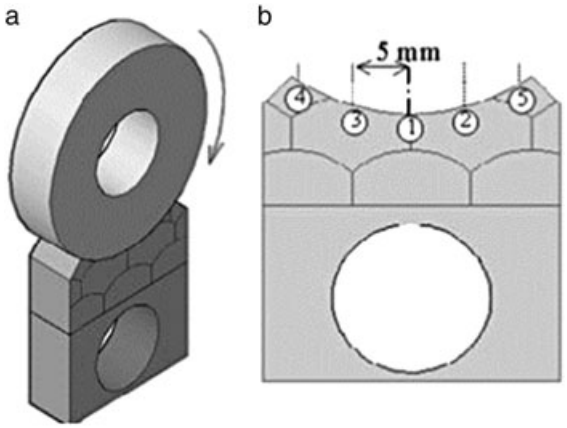

Figure 2. (a) Arrangement of the wear pair specimens and (b) location of the hardness measurements.

DOI: 10.1002/ls

balance. Hardness (HV1) was measured for each condition, as indicated in Figure 2b. After the tests, a hardness profile (HV0.05) was also obtained from the worn surface up to a depth of 1200 µm.

Surface roughness was measured by means of a Hommelwerke T-1000 roughness tester. Measurements were made on the surface of the wear tested samples with different conditions of load (500, 1250 and 2000 N). Obtained results corresponded to average roughness (*Ra*) over a measured length of 4.8 mm.

Wearing behaviour was studied in terms of the distance travelled by the wheel sliding on the plate; the weight loss was determined for 75, 550, 825, 1100, 1375, 1650, 3300 and 4950 m of travel distance. The friction coefficient was also measured for all loading conditions. Two sets (sample wheel) were tested for each condition and the results averaged. The produced debris was collected in each case. The temperature was measured after one hour of continuous testing using a thermocouple located 1 mm far from the contact area between both surfaces. Finally, worn surfaces and cross sections were observed by means of light and electron microscopy to determine the wear mechanisms involved.

RESULTS AND DISCUSSION

Macrostructure Characterisation

Figure 3a shows the welded coupon and Figure 3b a cross section of the welded specimen where the base metal, the weld deposit (hardfacing) and absence of macroscopic defects (pores, slag inclusions, cracks, etc.) can be observed. These data were confirmed by radiographic testing.

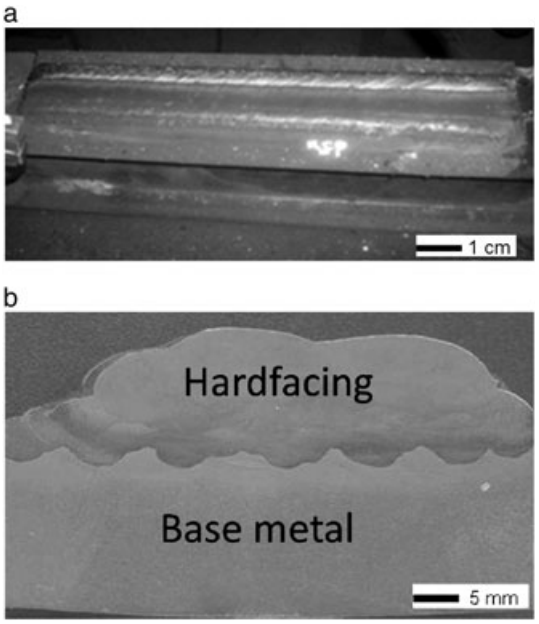

Figure 3. (a) A welded coupon and (b) its transversal sections.

DOI: 10.1002/ls

Chemical Composition

Table II shows the chemical composition results, measured on the surface of the last bead by means of spark emission spectrometry. Results complied with the manufacturer's specifications.

It is seen that the deposit corresponds to a Cr–Mo–V–W alloy, similar to the AISI H13 steel.

Microstructure

The microstructure for the AW condition (Figure 4a) was mainly composed of martensite (M) with some retained austenite (γ), with a dendritic segregation pattern; these observations were consistent with what was expected for these types of materials.[7,10,11] In addition, given the increase of alloy content detected in the interdendritic area,[10] the martensitic transformation start temperature (Ms) was locally reduced; this fact caused the appearance of retained austenite in the segregated regions.[5] On the other hand, and due to the fact that the deposit was welded in multi-passes, precipitation of small carbides was produced.[11]

Post-welding heat treatment caused carbide precipitation and transformation of retained austenite into tempered martensite. The content of retained austenite was reduced from 16% to 8%. This can be corroborated in Figure 4a and 4b. In previous works, the authors identified carbides of types $M_{23}C_7$, M_7C_3, M_2C and MC.[12]

Table II. All weld metal chemical composition (% in weight).

C	Mn	Si	Cr	Mo	V	W
0.48	1.30	0.67	5.5	2.5	0.4	1.9

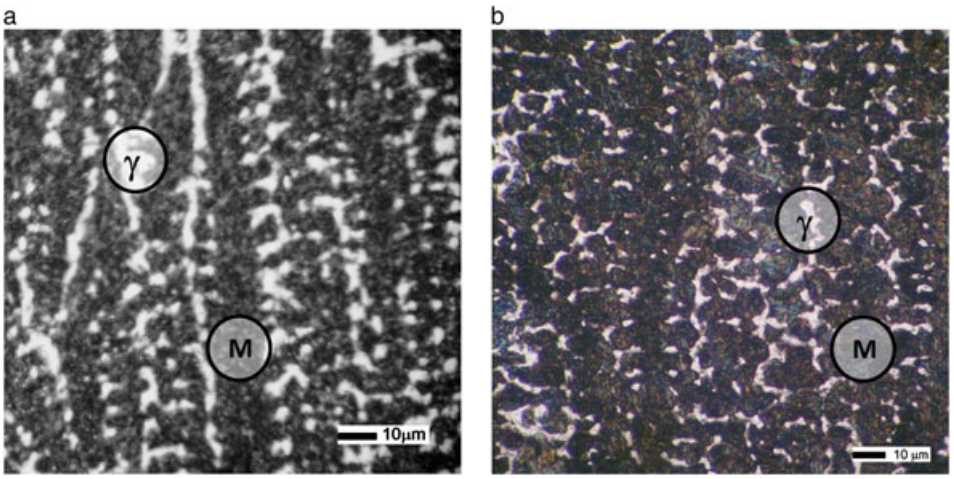

Figure 4. Microstructures of the (a) as-welded and (b) tempered samples at 550°C.

DOI: 10.1002/ls

Hardness

The samples before being wear tested. Hardness measurements of the AW and heat-treated specimens were 640 and 740 HV, respectively. The hardness increase with heat treatment was caused by coherent carbide precipitation that generated secondary hardening.

Worn surfaces. Figure , 5a, 5b and 5c shows the hardness variation versus the distance from the worn surface, for the AW and post-welding heat-treated (PWHT) samples, after testing with different loads. Figure 5a and 5b shows martensite hardening near the worn surface caused by plastic deformation. The temperature reached, between 100°C and 400°C, favoured deformation and hardening.[13] The observed hardening increased with the load applied during the test. The hardening of the surface was similar for both conditions (AW and PWHT). This hardened microstructure additionally acted as a support or base for oxide layer formation. Furthermore, it was observed that the zone affected by wear test was around 50 μm of depth from the surface.

The samples tested at 2000 N, Figure 5c, experienced a microstructure tempering caused by the temperature reached, which was 520°C at 1 mm from the contact area. It was also observed that on the surface of the heat-treated specimens, hardness was 896 HV and corresponded to the oxide formed on the surface.[14,15] The formation of this oxide layer was a result of both the high initial hardness

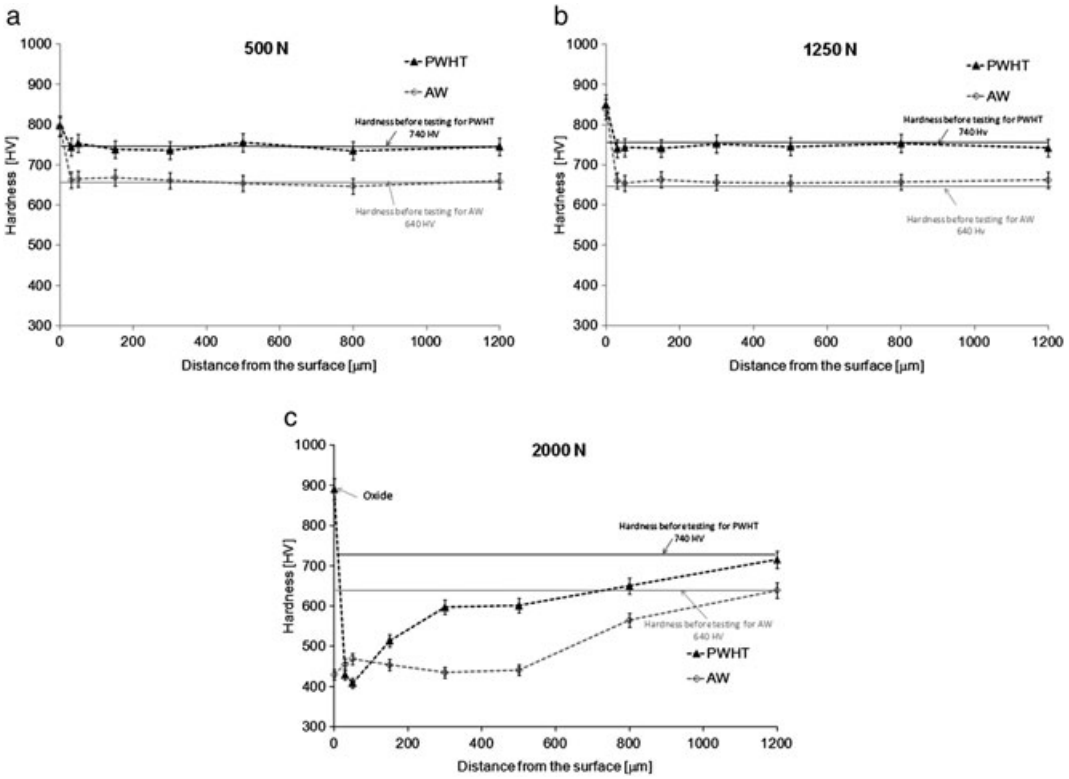

Figure 5. Hardness for the wear-tested samples at (a) 500, (b) 1250 and (c) 2000 N.

DOI: 10.1002/ls

microstructure that served as base or support and the temperature generated by friction.[16] The zone affected by the wear test was around 1200 μm of depth from the surface.

Wear

The wear rate was calculated from experimental results in terms of weight loss over the travelled distance. Figure 6 presents the results obtained for each condition.

Samples tested at 500 N showed that the AW specimens were more resistant to wear than the PWHT samples. This might be associated with the fact that during heat treatment, the chromium in the solution precipitated, forming carbides and therefore reducing the matrix resistance to oxidisation.[17,18] Oxide islands were found in worn surfaces of these samples, as can be seen in Figure 7a. Figure 7b shows EDS performed on zone A (oxide presence was confirmed by the EDS study). Abrasion lines, with orientation parallel to the sliding direction, were seen on the worn surfaces. These lines were produced by the rubbing of the hard zones of the wheel during sliding.[19–21] The predominant wear mechanism was mild oxidative, promoted by the test conditions (low load and low speed); the oxidation resistance of the material could have controlled the wear rate, with the hardness not being determinant.[12] Figure 7c shows an XRD pattern obtained from the worn surface of AW sample tested under 500 N. It was found that the austenite retained on the surface was totally transformed and that, furthermore, oxide of the Fe_2O_3 type partially covered the worn surface.

Figure 8a shows a scanning electron microscopy (SEM) image of debris collected for 3320 m of travel distance, corresponding to the PWHT specimen, tested under 500 N. The presence of oxides was determined through EDS (Figure 8b) and XRD (Figure 8c). The particles observed in Figure 8a could be divided into two groups according to their sizes. Large particles, of the order of 100 μm, with a plate shaped from the reference material and small particles, of the order of 10 μm, from the hardfacing material (as determined with EDS, Figure 8b) were found.[22] On the XRD pattern, the presence of Fe_2O_3 in the debris could be identified.

Samples tested at 2000 N showed that the PWHT coupons had better resistance to wear than the AW ones. This was likely related to the higher plastic deformation substrate in the AW samples, therefore producing a larger number of surface cracks parallel to the sliding direction (Figure 9a) that propagated until reaching a critical length and coming off as debris material afterwards.[23–25] In turn, the material

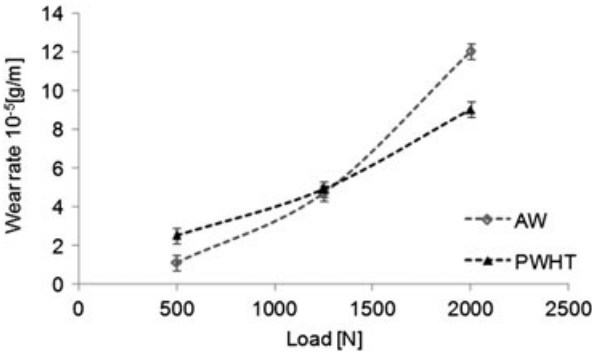

Figure 6. Wear rate for all the tested samples.

DOI: 10.1002/ls

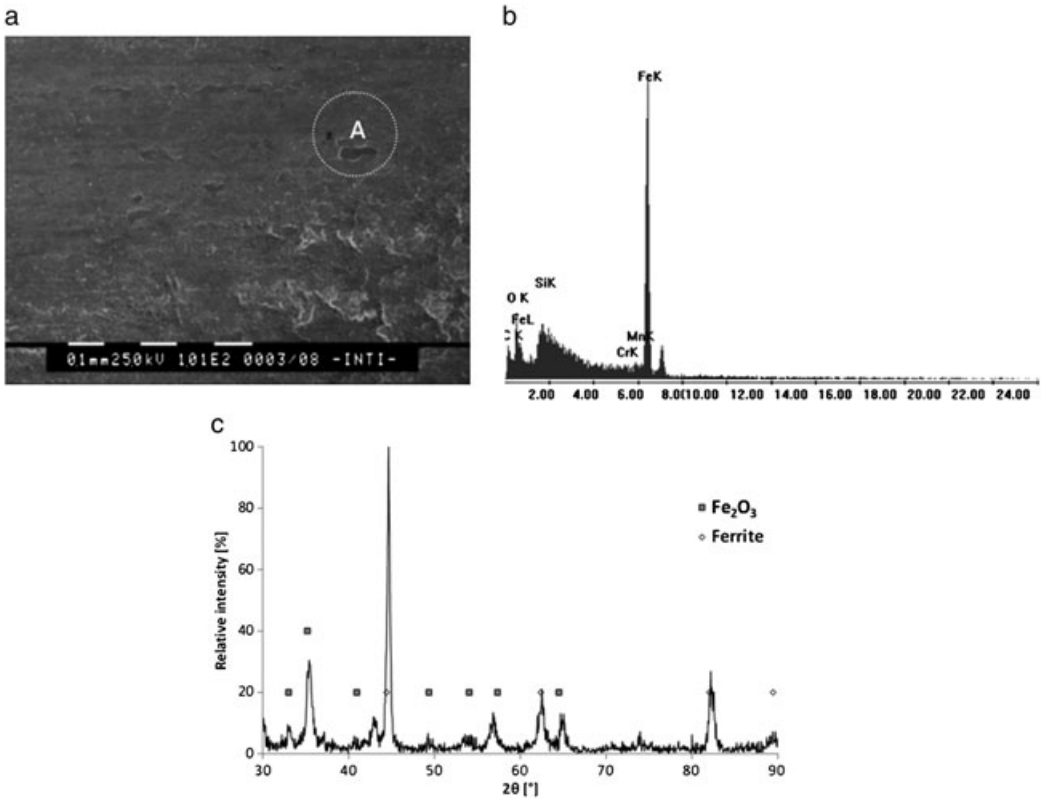

Figure 7. (a) Top view of the worn surface of an as-welded (AW) sample tested at 500 N, (b) energy dispersive X-ray spectroscopy of zone A and (c) X-ray diffraction of the worn surface of the AW sample tested at 500 N.

with the harder substrate allowed the formation of an oxide layer that rendered improved resistance to wear; see Figure 9b.[23,26]

X-ray diffraction was performed on the worn surface to identify the oxides formed during the wear process. It was observed that the retained austenite on the surface was fully transformed and that oxides of the Fe_2O_3 and Fe_3O_4 types partially covered the worn surface (Figure 10a and 10b), both factors improving wear resistance.[20] The predominant wear mechanism was severe oxidative.

Figure 11a shows a SEM image of debris collected for 3320 m of travel distance, corresponding to the PWHT specimens, tested at 2000 N. The observed particles were large, of the order of 100 μm with a plate shape. In the XRD pattern (Figure 11b), the presence of Fe_2O_3 and Fe_3O_4 was detected.

The coupons tested at 1250 N showed both wear regimes, mild oxidative and severe oxidative, being the transition zone between both wear mechanisms.

Friction

The friction coefficient for all tested samples was found to vary between 0.3 and 0.4. Figure 12 shows that for coupons tested at 500 N and 1250 N, the samples with higher oxidation were those that

DOI: 10.1002/ls

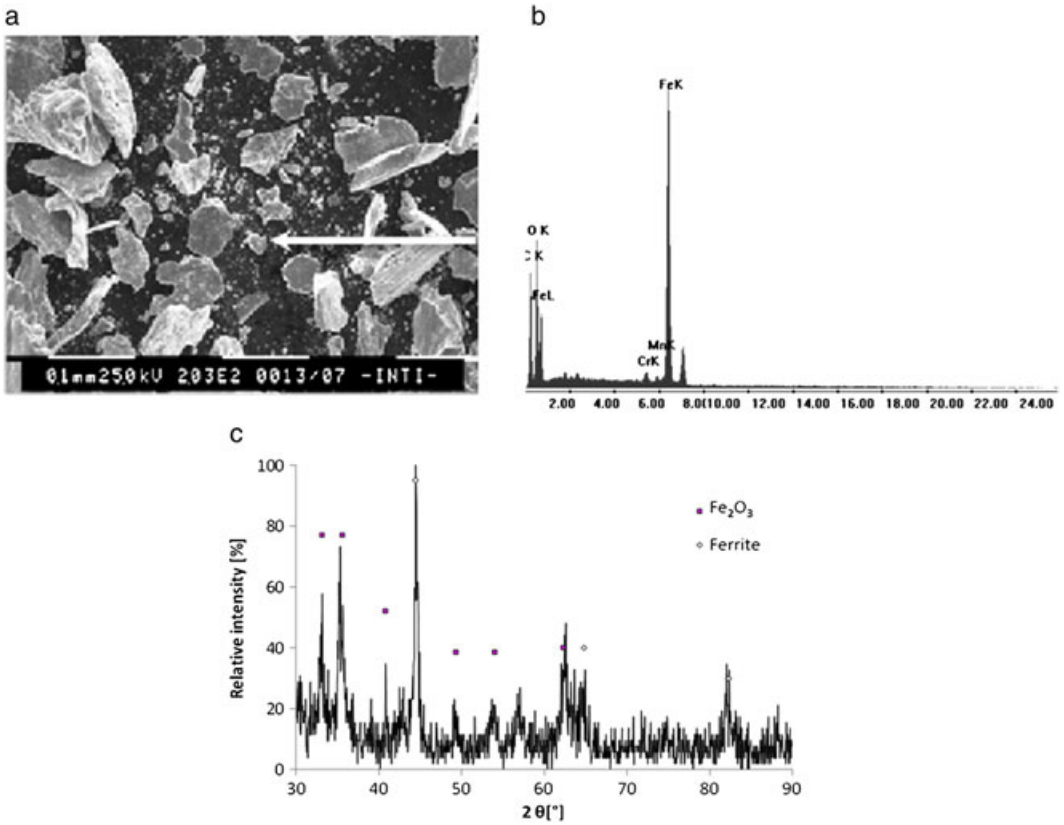

Figure 8. (a) Scanning electron microscopy image of a debris collected from the as-welded sample tested at 500 N, (b) energy dispersive X-ray spectroscopy of a selected particle and (c) X-ray diffraction patterns of this debris.

presented lower friction coefficients and, as previously discussed, were the most heavily worn. This might be related to the fact that with a larger surface covered by oxides, metal contact would be reduced and therefore the lower would be the sliding force and the friction.

When the applied load was increased to 2000 N, the wear mechanism turned into delamination or severe oxidation; the friction coefficient was lower for the AW condition. This might be related to the type and thickness of the oxide formed on the surface,[26] which might have acted as lubricant, reducing the friction coefficient. As all the worn coupons were covered with oxide, the loosening of the oxide layer might have contributed to the mentioned lubrication effect, as previously shown by So and Munther.[26,27]

Figure 13 shows the accumulated oxide before the contact area between the two pieces. Under certain size and hardness oxide conditions, part of this oxide might have entered the contact area and produced an abrasive effect, increasing locally the friction coefficient.[28]

DOI: 10.1002/ls

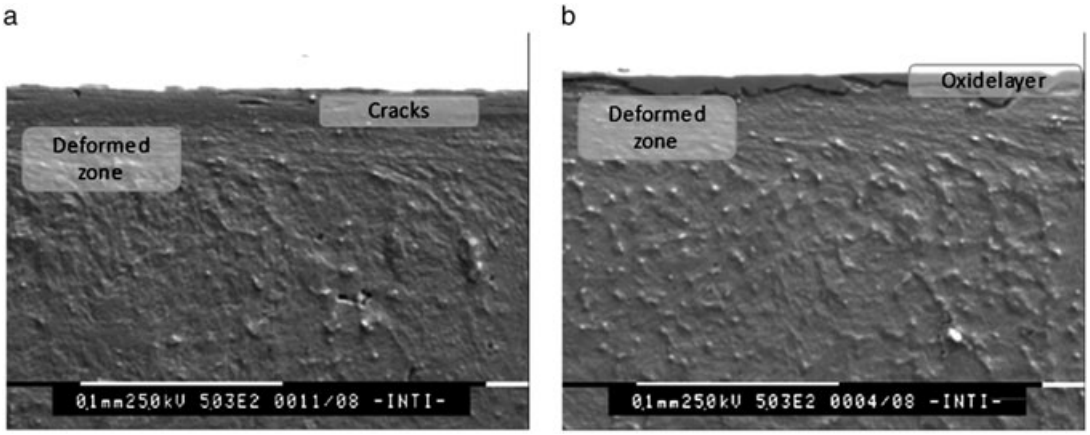

Figure 9. Scanning electron microscopy images of the (a) as-welded and (b) post-welding heat-treated tested samples at 2000 N.

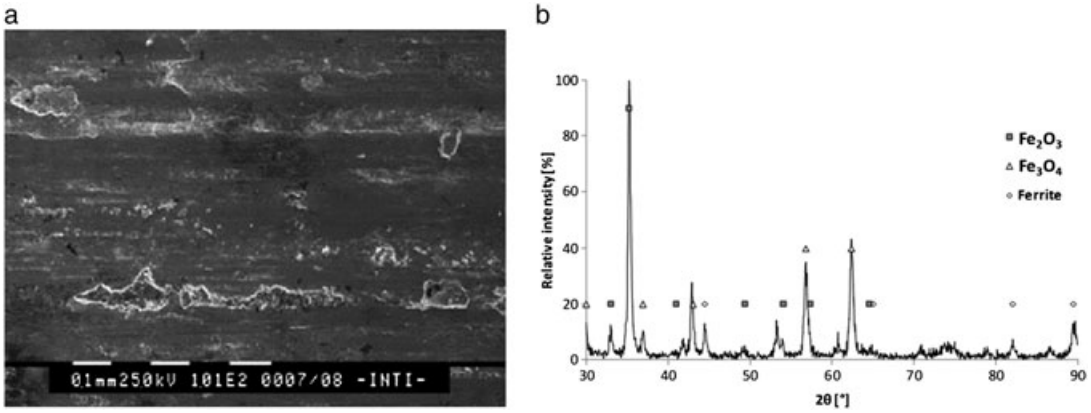

Figure 10. (a) Top view and (b) X-ray diffraction of the worn surface of the post-welding heat-treated sample tested at 2000 N.

Roughness

The roughness of machined specimen surface was 0.8 μm. After the wear tests, roughness evolved according to the applied load as indicated in Figure 14.

As-welded samples presented lower roughness at 500 N and 1250 N loads. This might be linked to a less severe wear condition in these samples, due to their improved resistance to oxidation (higher chromium in solution) resulting in reduced damage. On the other hand, in samples tested with 2000 N load, heat treatment favoured the formation of a continuous oxide layer that helped the development of an improved resistance to wear and less roughness.[29]

DOI: 10.1002/ls

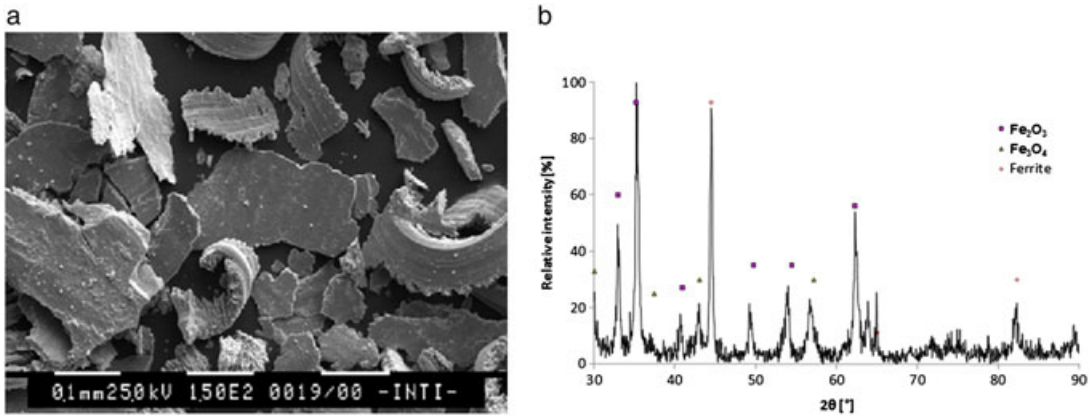

Figure 11. (a) Scanning electron microscopy image of a debris collected from the post-welding heat-treated specimens tested at 2000 N and (b) X-ray diffraction patterns of this debris.

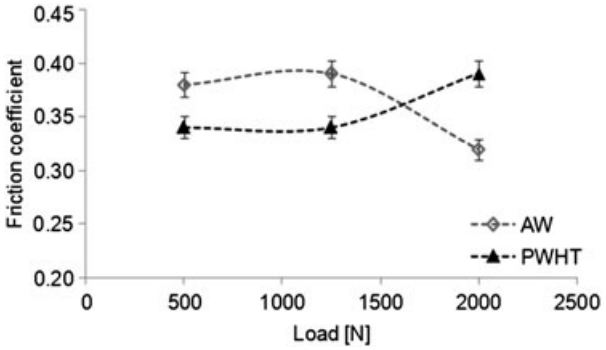

Figure 12. Friction coefficient for all the samples.

CONCLUSION

For all conditions, the microstructure was composed mainly of martensite with some retained austenite, with a dendritic segregation pattern. The samples treated at 550°C showed a secondary hardening effect accompanied by the transformation of retained austenite into martensite, which resulted in an increase in hardness when compared with the AW material.

The specimens tested at 500 and 1250 N of applied load showed hardening in the sub-surface region. At 2000 N, the weld metal experienced softening in this region due to the tempering of the martensite caused by the high surface temperature. On the heat-treated samples, a hard oxide layer was detected after wear test.

Wear of specimens in pure sliding conditions by Amsler testing at loads of 500, 1250 and 2000 N showed a linear relationship between the weight loss and the travelled distance. Oxidation and plastic deformation was visible at worn surfaces of the tested samples. At low loads, wear regime was mild

DOI: 10.1002/ls

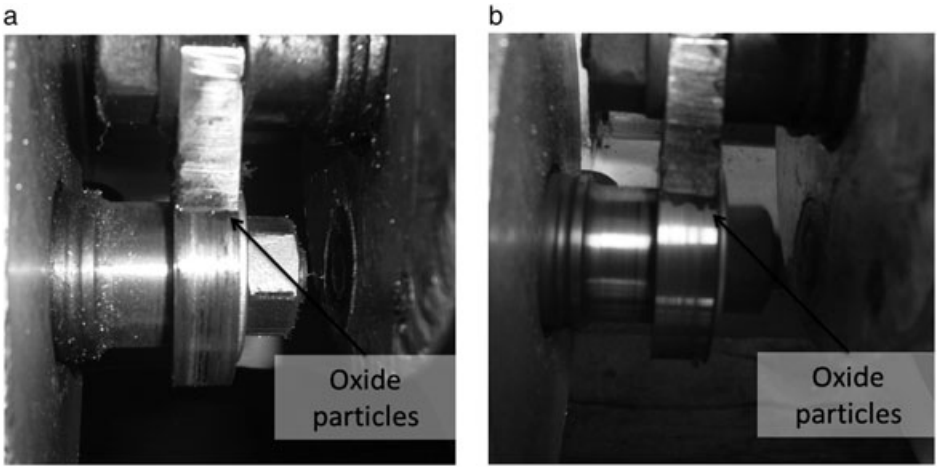

Figure 13. Images taken during the friction test at (a) 500 and (b) 2000 N.

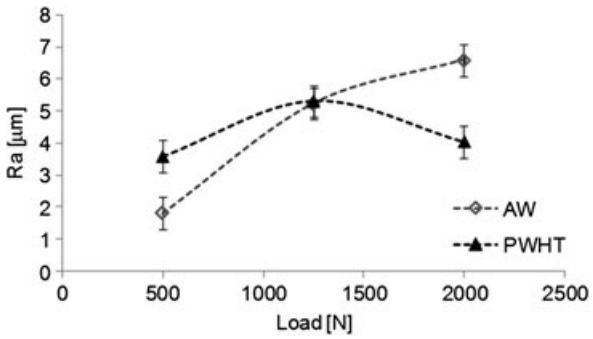

Figure 14. Roughness on the surfaces of the tested coupons.

oxidative; the AW condition presented improved wear resistance and a higher friction coefficient than the PWHT specimens. At higher loads, deformation resistance of the substrate was determinant for wear. The wear regime was severe oxidative. Heat-treated samples presented higher resistance to wear and a higher friction coefficient.

The application of post-welding heat treatment for this material must be carefully analysed, especially in low load services, because it could be deleterious for wear resistance.

ACKNOWLEDGEMENTS

The authors wish to thank Eutectic-Conarco Argentina for the provision of the consumable used in this work; to ESAB Brazil for the manufacturing of the consumable, which was especially produced for this investigation; to Air Liquide Argentina for the free supply of welding gases; Conarco-ESAB Argentina Industrial Applications Workshop for the support with the welding of the samples; to Conarco-ESAB

DOI: 10.1002/ls

Argentina for conducting chemical analyses; to INTI-Mechanical Laboratory for the facilities of scanning electron microscopy and to APUEMFI (Association of Teachers of Mechanics from the National University of Lomas de Zamora) for the financial aid in this project. The ANPCyT (National Agency for the Promotion of Science and Technology) is also recognised herein for their financial support.

REFERENCES

1. Merrick S, Kotecki D, Wu J. *Materials and Applications — Part 2* (8th edn), Welding Handbook. American Welding Society 1998: 422.
2. Huisman MD. Flux- and metal-cored wires, a productive alternative to stick electrodes and solid wires. *Svetsaren* 1996; **1–2**:6–14.
3. Lyttle KA. Metal cored wires: where do they fit in your future? *Welding Journal* 1996; **75**(10):35–38.
4. Myres D. Metal cored wires: advantages and disadvantages. *Welding Journal* 2002; **81**(9):39–42.
5. Wu W, Hwu LY, Lin DY, Lee JL. The relationship between alloying elements and retained austenite in martensitic stainless steel welds. *Scripta Materialia* 2000; **42**:1071–1076.
6. Koteki D, Ogborn J. Abrasion resistance of iron-based hardfacing alloys. *Welding Journal* 1995; **74**(8):269s-278s.
7. Bortoni OE, Patrone JJ, Marino PS. Recargue por soldadura de superficies sometidas a desgaste. *Siderurgia* 1989; **49**:114–139.
8. Gualco A, Svoboda H, Surian E, Devedia L. Effect of post-weld heat treatment on wear resistance of martensitic steel hard-facing deposits. *Soldagem & Inspeçao* 2008; **13**(3):237–244.
9. Cullity BD, Stock SR. *Elements of X-ray Diffraction*. Prentice Hall 2001: 347–361.
10. Gualco A, Svoboda H, Surian E, Ramini M, De Vedia L. *Dilution Study in Hardfacing Deposits (in Spanish)*. SAM-CONAMET: Mar del Plata 2005.
11. Leshchinskiy LK, Samotugin SS. Mechanical properties of plasma-hardened 5% chromium tool steel deposited by arc welding. *Welding Journal* 2001; **80**(1):25–30.
12. Gualco A, Svoboda H, Surian E, De Vedia L. Effect of welding procedure on wear behaviour of a modified martensitic tool steel hardfacing deposit. *Materials and Design* 2010; **31**(9):4165–4173.
13. Tuckart W, Iurman L, Forlerer E. *Influencia de la microestructura sobre las capas tribologicamente mezcladas protectoras (in Spanish)*. SAM/CONAMET: Argentina 2009.
14. Barrau O, Boher C, Vergne C, Rezai-Aria F. Investigations of friction and wear mechanisms of hot forging tool steels. *Proceedings of the 6th International Tooling Conference*, 2002.
15. Baque P, Fernier P. Contribution des oxydes mètalliques au frottement à sec. Note Technique CETIM, vol. **12**, 1975.
16. Wang Y, Lei T, Liu J. Tribo-metallographic behavior of high carbon steels in dry sliding III. Dynamic microstructural changes and wear. *Wear* 1999; **231**:20–37.
17. Eyre TS, Maynakd D. Surface aspects of unlubricated metal-to-metal wear. *Wear* 1971; **18**:301–310.
18. Vardavoulias M. The role of hard second phases in the mild oxidational wear mechanism of high-speed steel-based materials. *Wear* 1994; **173**:105–114.
19. Wang Y, Lei T, Liu J. Tribo-metallographic behavior of high carbon steels in dry sliding II. Microstructure and wear. *Wear* 1999; **231**:12–19.
20. Fontalvo GA, Mitterer C. The effect of oxide-forming alloying elements on the high temperature wear of a hot work steel. *Wear* 2005; **258**:1491–1499.
21. Quinn TFJ. The role of oxidation in the mild wear of steel. *British Journal of Applied Physics* 1962; **13**:33–46.
22. Bahrami A, Anijdan SHM, Golozar MA, Shamanian M. Effects of conventional heat treatment on wear resistance of AISI H13 tool steel. *Wear* 2005; **258**:846–851.
23. Cui XH, Wang SQ, Wang F, Chen KM. Research on oxidation wear mechanism of the cast steels. *Wear* 2008; **265**:468–476.
24. Hurricks PL. Some aspects of the metallurgy and wear resistance of surface coatings. *Wear* 1972; **22**(3):291–320.
25. Suh NP. The delamination theory of wear. *Wear* 1973; **25**:111–124.
26. So H, Yu DS, Chuang CY. Formation and wear mechanism of tribo-oxides and the regime of oxidational wear of steel. *Wear* 2002; **253**:1004–1015.
27. Munther A, Lenard JG. The effect of scaling on interfacial friction in hot rolling of steels. *Journal of Materials Processing Technology* 1998; **88**:105–113.
28. Larsen-Basse J. *Flux Cored Arc Welding*. ASM-Metals Handbook: Friction, Lubrication and Wear Technology, vol. **18**: ASM. 12–40. 1992.
29. Menezes P, Satish K, Kailas V. Effect of surface roughness parameters and surface texture on friction and transfer layer formation in tin–steel tribo-system. *Journal of Materials Processing Technology* 2008; **208**:372–382.

DOI: 10.1002/ls